Characterization Study of Neck Photoplethysmography

Irene García-López, Syed Anas Imtiaz and Esther Rodriguez-Villegas

Abstract— **This paper presents a comparison between finger and neck photoplethysmography (PPG) in order to assess the potential and limitations of this, non-conventionally used, body site for application in pulse oximetry. PPG signals were recorded at both sites from healthy subjects to inspect the differences in average waveforms, as well as in oxygen saturation (SpO_2) and heart rate (HR) estimation. The results show significant differences in the average PPG pulse waveforms for different contour features such as diastolic or dicrotic notch amplitude, among others. The results show that the HR estimated from signals obtained with the neck sensor are strongly correlated to the output of the reference finger (R=0.862, MAE=1.27 BPM), whereas SpO_2 measurements are not that accurately predicted (R=0.129, MAE=11.7%). Spectrograms under different breathing conditions revealed that the respiratory frequency is more predominant in neck PPG than in finger, which has a great potential for respiratory rate (RR) extraction. These are very promising results for the suitability of the neck as an alternative location for monitoring of respiratory diseases, and specifically for sleep apnea.**

I. Introduction

Photoplethysmography (PPG) is a non-invasive optical technique measuring changes in blood volume at the skin surface [1]. Pulse oximeter sensors are used to extract the PPG signal relying on the difference in light absorption properties of the microvasculature of tissues. Oxyhemoglobin absorbs more infrared (940 nm) and less red light (660nm) in comparison to deoxyhemoglobin, which allows fluctuations of oxygenated arterial blood to be observed [2]. The technology consists of a red and an infrared light-emitting diodes (LEDs) that illuminate the tissue, and a photodetector that senses light intensity output variations. The resulting PPG waveform shows two principal constituents. An AC pulsatile component of around 1 Hz frequency, reflects the arterial pulsations at each heartbeat such that each pulse is characterized by a systolic and diastolic peak. A DC component accounts for light interactions with non-pulsatile arterial, venous blood and other non-vascular tissues [3]. The applications of PPG are numerous, but vital cardio-respiratory parameters such as peripheral oxygen saturation (SpO_2), heart rate (HR) or respiratory rate (RR) are usually of primary interest [4]. Two types of contact PPG exist: transmission and reflectance. Transmission PPG is generally used in fingertip commercial pulse oximetry. In the latter the light emitted by the LEDs is transmitted across the tissue before being sensed by the photodetector on the other side. The finger is considered the gold standard measurement site because it provides large capillarity, and a practical stable attachment. Reflectance PPG can be used in a wider range of measurements sites, since the photodetector is placed alongside the LEDs to detect the light reflected from superficial vessels. Some examples of wearable devices implementing reflectance PPG are: earlobe magnetic earrings [5], wrist-watch PPG sensor [6], or forehead wireless-based reflectance sensors [7]. An alternative positioning could also be the neck, but the characteristics of the signal in this location have not been explored. The neck, however, could offer great benefits over conventional finger PPG in the context of some diseases for which additional physiological biomarkers are desired to be recorded simultaneously with the same wearable system. Specifically, for respiratory diseases such as sleep apnea, the neck offers a unique location for cardio-respiratory multimodal signal acquisition [8]. The only work reported on PPG acquisition from the neck focused on showing the feasibility of extracting PPG from this site [9], and on determining the most stable position for acquisition of the signal [10]. None of these works studied the actual characteristics of the signal. This is necessary, however, not only to correctly interpret and potentially extract new diseases indicators, but also to develop targeted signal processing techniques to eliminate artifacts that could possibly disrupt the PPG signal. This paper aims to compare finger and neck PPG signals in order to characterize this novel measurement site for different breathing, and assess the potentials and limitations for its application in pulse oximetry.

Research supported in part by "La Caixa" Foundation and in part by the Engineering and Physical Sciences Research Council (EPSRC), UK / grant agreement no. EP/P009794/1.

I. García-López, S. A. Imtiaz and E. Rodriguez-Villegas are with the Wearable Technologies Lab, Department of Electrical and Electronic Engineering, Imperial College London, SW7 2BT, United Kingdom. E-mail: {irene.garcia-lopez15, anas.imtiaz, e.rodriguez}@imperial.ac.uk

II. Methods

A. Data collection

Signals from a total of 9 healthy subjects (5 males and 4 females), with average age 25 $\pm$ 2 years old, height of 1.75 $\pm$ 0.12 m and weight of 70 $\pm$ 15 kg, were acquired. The study was approved by the Local Ethics Committee of Imperial College London (ICREC ref.: 18IC4358), and written informed consent was obtained from all subjects. Participants lied down in a supine position to simulate sleeping conditions and wore two sensors simultaneously for data acquisition. One reflectance pulse oximeter sensor (8000R, Nonin) coupled to an OEM processing module (Xpod, Nonin), was located in the suprasternal notch of the neck. A transmission finger pulse oximeter (Onyx II 9560, Nonin) with Bluetooth connectivity, was located in the index finger of the left hand as reference. PPG signals were acquired at a sampling frequency of 75Hz. Four-beat average SpO_2 and HR measurements were also output every 1/3 of

a second. Data acquisition of both sensors was synchronized in MATLAB. Four 140s recordings were carried out at rest, under different breathing conditions, as shown in Fig. 1.

Participants were initially asked to breathe at their normal pace for the whole duration of the recording. Then they had to introduce three alternating fast breathing intervals of 20s each. Later, they changed the breathing frequency to a slow controlled rate for two intervals of respectively 30s and 40s, to clearly observe the changes in respiration frequency with respect to the normal reference pace. Finally, they held their breath for three intervals of 20s, to simulate apnea events.

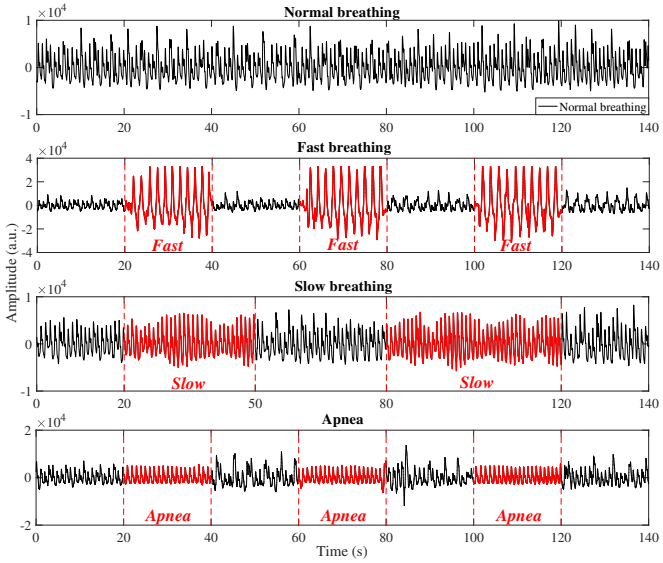


Fig. 1. Normal, fast and slow breathing PPG recordings at the neck. In black breathing at normal pace. In red, breathing with altered frequency.

B. SpO_2 and HR measurements analysis

We investigated the accuracy of the neck reflectance sensor in the estimation of SpO_2 and HR measurements, taking as reference the finger sensor. Average mean absolute errors (MAE) and correlation coefficients were calculated.

C. Average waveforms characteristics

The PPG neck waveform of the normal breathing signal was compared to the gold standard finger PPG one, with time domain features.

1) Automated pulse segmentation and waveform averaging: The PPG signal was first filtered to remove the DC and low frequency components, with a fourth order high pass Butterworth filter with 0.7Hz cut off frequency. In order to detect the onsets of each pulse, the lower peak envelope of the PPG signal was determined using spline interpolation over local maxima separated by a time window of 0.667s. The maximum between successive troughs was selected as the systolic peak. Wrongly segmented pulses with a duration greater than the mean pulse duration by three standard deviations were discarded. Subsequently, a normalization in time and amplitude was performed for each of the remaining pulses. Pulses were aligned by calculating a delay shift for

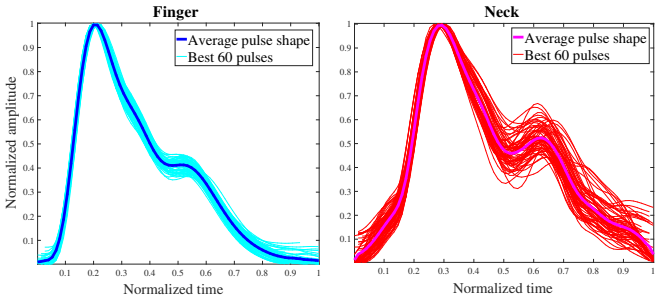


Fig. 2. Average finger and neck PPG pulse waveforms for one participant.

each pulse that maximized the overall correlation among all pulses. The first approximation of the mean pulse waveform was then obtained by averaging point by point. The 60 beats with the shortest Euclidean distance to the mean waveform were then selected. Taking into consideration this final set of good quality pulses, the definitive average normal pulse waveforms of the finger and the neck were extracted for each subject. This can be observed in Fig. 2.

2) Feature extraction: As shown in Fig. 3, in order to obtain the morphological characteristics of the average normal pulse waveforms, the systolic peak was detected with the maximum of the mean pulse, the dicrotic notch with the second maximum of the second derivative, and the diastolic peak with the minima right after this maximum. The features extracted for finger and neck average pulse waveforms comparison, are described in Table I.

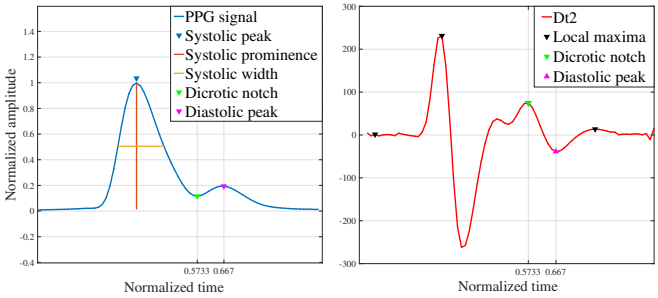


Fig. 3. Average pulse waveform and the its second derivative, for diastolic and dicrotic notch detection.

3) Statistical tests: The non-parametric Wilcoxon signed-rank test was used for the pairwise comparisons of the features since the number of samples was too small and the population was not normally distributed. This tested for the null hypothesis that data in finger and neck PPG signals are samples from continuous distributions with equal medians, against the alternative. Median values of each feature, as well as the interquartile range (IQR) variability, are reported.

D. Spectrograms for different breathing conditions

Finger and neck PPG spectrograms for normal, fast, slow and apnea breathing conditions were computed using the squared magnitude of the Short-Time Fourier Transform (STFT), with a window of 15s and an overlap of 90%. Normalized spectrograms of each sensor were subtracted to inspect the differences in power between them.

TABLE I

WILCOXON SIGNED-RANK TEST PAIRWISE COMPARISONS BETWEEN FINGER AND NECK FOR THE DIFFERENT FEATURES (***P<0.05**)

Features	*Finger*		*Neck*		*Definition*
	Median	IQR	Median	IQR	
Systolic Peak Prominence*	**0.985**	**0.008**	**0.937**	**0.074**	measured by how much the systolic peak stood out due to its intrinsic height and its location relative to the diastolic peak [11].
Systolic Peak Time	0.267	0.107	0.327	0.140	time at which the systolic peak occurred in the normalized time of 1 second.
Systolic Peak Width*	**0.242**	**0.087**	**0.324**	**0.120**	computed as the distance between the points to the left and right of the systolic peak measured at half prominence height [11].
Diastolic Peak Amplitude*	**0.293**	**0.125**	**0.500**	**0.149**	corresponded to the normalized height of the second peak in the PPG pulse waveform.
Diastolic Peak Prominence	0.035	0.072	0.026	0.101	measured by how much the diastolic peak stood out due to its intrinsic height and its location relative to the systolic peak [11].
Diastolic Peak Time	0.620	0.080	0.647	0.093	time at which the diastolic peak occurred in the normalized time of 1 second.
Diastolic Peak Width	0.076	0.086	0.036	0.101	computed as the distance between the points to the left and right of the diastolic peak measured at half prominence height [11].
Pulse Propagation Time (PPT)	0.333	0.047	0.307	0.047	time difference between the occurrence of the systolic and diastolic peaks.
Pulse Kurtosis	2.694	1.234	2.092	0.660	referred to the degree of peakedness of the pulse [12].
Pulse Skewness*	**0.898**	**0.600**	**0.482**	**0.476**	referred to the degree of symmetry of the pulse [12].
Augmentation Index (AI)*	**0.706**	**0.123**	**0.496**	**0.149**	ratio between the difference in heights of the systolic (s) and diastolic (d) peaks in relation to the systolic peak height [4]: $AI = (s-d)/s$.
Stiffness Index (SI)	5.250	0.648	5.674	0.879	indicates arterial distensibility, can be defined as the ratio between height (h) and PPT [13]: $SI = h/PPT$.
Total Pulse Area*	**0.321**	**0.081**	**0.419**	**0.072**	the area under the pulse curve from onset to offset.
Systolic Area (A1)*	**0.246**	**0.061**	**0.304**	**0.051**	area under the pulse curve from the onset until the dicrotic notch.
Diastolic Area (A2)*	**0.066**	**0.028**	**0.109**	**0.039**	area under the pulse curve from the dicrotic notch until the offset.
Inflection Point Area (IPA)*	**0.262**	**0.092**	**0.365**	**0.246**	ratio between the diastolic and systolic areas: $IPA = A2/A1$. It is an indicator of pulse wave reflection [4].
Dicrotic Notch Amplitude*	**0.285**	**0.200**	**0.496**	**0.128**	normalized height of the inflection point between the systolic and diastolic peaks.
Dicrotic Notch Time	0.533	0.087	0.547	0.127	time at which the dicrotic notch occured in the normalized time of 1 second.

III. RESULTS AND DISCUSSION

A. Finger and neck normal PPG signals comparison

1) SpO_2 and HR measurements: The differences in the estimation of SpO_2 and HR over time between the two sensors can be observed in Fig. 4. A summary of the average MAE and correlation coefficient for all subjects is presented in Table II. The HR values measured by the neck sensor follow very closely the variations of the reference finger pulse oximeter over time. The correlation coefficient between them was found to be R=0.862 for all subjects. The average MAE between the neck reflectance sensor and the reference finger sensor is 1.27BPM. This very low error and the strong correlation demonstrate the potential of the neck as a signal monitoring location to reliably extract the pulse rate from the PPG signal. The SpO_2 estimation by the neck PPG sensor was not as accurate, as the average MAE resulted in 11.7% error and there was no correlation (R=0.129). This could be explained by the fact that different body parts have different capillarity and tissue characteristics, showing variations in the reflected light optical path. Since the sensor placed at the neck was not specifically calibrated for this body region, the PPG signals obtained from the neck need to be further studied to develop a wearable sensor with specific signal processing algorithms for a more precise SpO_2 calculation.

2) PPG average waveforms morphological characteristics: Based on the results from the Wilcoxon signed-rank test, the neck PPG average pulse was significantly different from the finger standard pulse waveform for different features. This can be seen in bold in the comparison of median values in Table I. Based on these, the neck waveform shows a significantly lower systolic peak prominence, pulse skewness and AI than the finger one. The neck pulse also exhibits a significantly greater systolic peak width, diastolic peak amplitude, pulse area, IPA, A1, A2 and dicrotic notch amplitude than the finger PPG. Overall, the neck PPG pulse is less skewed than the finger PPG pulse. This is corroborated by the fact that the systolic peak prominence is lower since the dicrotic notch and diastolic peak heights are greater. As a consequence, A1 and A2 have increased, increasing the total area of the pulse. A possible interpretation for these changes in the PPG pulse contour is that, depending on

TABLE II

COMPARISON OF AVERAGE SpO_2 AND HR MEASUREMENTS FOR FINGER AND NECK PPG SENSORS FOR ALL PARTICIPANTS

	SpO_2(%)	Heart rate (BPM)
Mean absolute error (MAE)	11.7%	1.27 BPM
Correlation coefficient (R)	0.129	0.862

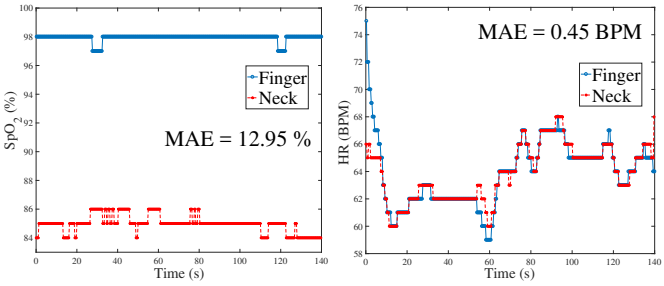


Fig. 4. Normal breathing SpO_2 and HR measurements comparison between finger and neck PPG sensors over time for one participant.

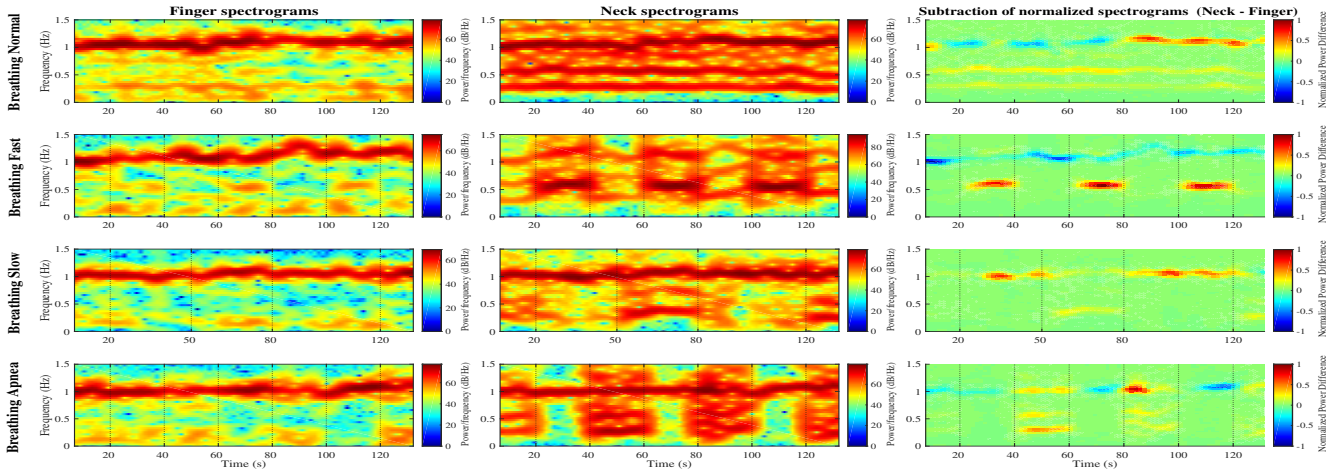


Fig. 5. Comparison of finger and neck spectrograms under different breathing conditions: normal breathing, fast breathing, slow breathing and apnea (absence of breathing). The difference between normalized power spectrograms for the neck and finger shows in hot colours a positive value of the power difference (Neck>Finger), and in cold colours a negative one (Neck<Finger).

the anatomical site, the reflection wave giving rise to the diastolic peak will be transmitted via different possible paths through the complex arterial tree. Thus, due to the proximity of the neck to the body trunk, the reflection wave arrives with greater amplitude since it has gone across less bifurcations than when traveling to the periphery.

B. Differences in normal, slow and fast breathing

Finger and neck spectrograms were also compared under different breathing conditions in the range of 0 to 1.5Hz frequencies, where the major distinctions appear. This has been shown in Fig. 5. In the case of finger, no matter under which breathing condition, the spectrograms show approximatively the same spectral components. A high concentration of power at the PPG fundamental frequency of 1Hz reveals the AC arterial pulsations. A reduced power density at low frequencies (around 0.26Hz) denotes the PPG DC component modulated by respiration. In contrast, for the neck, some differences can be noticed across different breathing situations. For normal breathing, the neck spectrogram coincides with the finger one for the major power band at 1Hz, but two other bands at low frequencies, 0.28Hz and 0.56Hz, stand out equally. These correspond to the fundamental frequency and the first harmonic of the respiration, which show higher power in the neck than in the finger, since the neck is more sensitive to movements of the thoracic cage. These results are very promising since it is easier to extract the respiratory rate at the neck than in typical finger pulse oximetry. During fast breathing, the main differences between the finger and neck spectral content are two high power bands at 0.55Hz and 1.1Hz. The predominance of the fast breathing fundamental frequency and its harmonics interfere with the normal PPG power spectrum. This can be a limitation for this new measurement site, as new filtering techniques will be needed to deal with artifacts, in order to correctly infer SpO_2. In the case of slow breathing, the respiration components are less predominant than for normal since the breathing was controlled. However, when apnea events are simulated, the respiration power bands completely disappear in the neck spectrogram whereas in the finger they remain present. This makes easier to identify the complete absence of respiration frequency and facilitates apnea identification. The potential of neck PPG for sleep apnea detection is therefore doublefold as, not only the decrease in SpO_2 levels can indicate hypoxia, but also the absence of respiration can be detected by examining the PPG power spectral content.

REFERENCES

[1] J. Allen, "Photoplethysmography and its application in clinical physiological measurement," *Physiological measurement*, vol. 28, no. 3, p. R1, 2007.

[2] J. E. Sinex, "Pulse oximetry: principles and limitations," *The American journal of emergency medicine*, vol. 17, no. 1, pp. 59–66, 1999.

[3] E. D. Chan, M. M. Chan, and M. M. Chan, "Pulse oximetry: understanding its basic principles facilitates appreciation of its limitations," *Respiratory medicine*, vol. 107, no. 6, pp. 789–799, 2013.

[4] M. Elgendi, "On the analysis of fingertip photoplethysmogram signals," *Current cardiology reviews*, vol. 8, no. 1, pp. 14–25, 2012.

[5] M.-Z. Poh, N. C. Swenson, and R. W. Picard, "Motion-tolerant magnetic earring sensor and wireless earpiece for wearable photoplethysmography," *IEEE Transactions on Information Technology in Biomedicine*, vol. 14, no. 3, pp. 786–794, 2010.

[6] Y. Lee, H. Shin, J. Jo, and Y.-K. Lee, "Development of a wristwatch-type ppg array sensor module," in *ICCE*. IEEE, 2011, pp. 168–171.

[7] W. Johnston and Y. Mendelson, "Extracting breathing rate information from a wearable reflectance pulse oximeter sensor," in *EMBC*, vol. 2. IEEE, 2004, pp. 5388–5391.

[8] E. Rodriguez-Villegas, G. Chen, J. Radcliffe, and J. Duncan, "A pilot study of a wearable apnoea detection device," *BMJ open*, vol. 4, no. 10, 2014.

[9] M. Peng, S. A. Imtiaz, and E. Rodriguez-Villegas, "Pulse oximetry in the neck-a proof of concept," in *EMBC*. IEEE, 2017, pp. 877–880.

[10] Y. Zhong, Y. Pan, L. Zhang, and K.-T. Cheng, "A wearable signal acquisition system for physiological signs including throat ppg," in *EMBC*. IEEE, 2016, pp. 603–606.

[11] Mathworks. Findpeaks. (Accessed: 2018-01-24). [Online]. Available: https://uk.mathworks.com/help/signal/ref/findpeaks.html

[12] R. Couceiro, P. Carvalho, R. P. Paiva, J. Henriques, and J. Muehlsteff, "Detection of motion artifact patterns in photoplethysmographic signals based on time and period domain analysis," *Physiological measurement*, vol. 35, no. 12, p. 2369, 2014.

[13] S. C. Millasseau, J. M. Ritter, K. Takazawa, and P. J. Chowienczyk, "Contour analysis of the photoplethysmographic pulse measured at the finger," *Journal of hypertension*, vol. 24, no. 8, pp. 1449–1456, 2006.